Available online at www.tox.or.kr

MCT

Differences in Gene Expression Profiles Reflecting Differences in Drug Sensitivity to Acetaminophen in Normal and Transformed Hepatic Cell Lines *In vitro*

Youn Kyoung Jeong[1,3], Jin Seok Kang[4], Joo Whan Kim[1], Soo Kyung Suh[1], Michael Lee[2], Seung Hee Kim[1], Sang Kook Lee[3] & Sue Nie Park[1]

[1]Division of Genetic Toxicology, National Institute of Toxicological Research, Korea Food and Drug Administration, Seoul 122-704, Korea
[2]Department of Biology, College of Natural Sciences, Incheon University, Incheon 402-749, Korea
[3]Department of Pharmacognosy, College of Pharmacy, Ewha Womans University, Seoul 120-750, Korea
[4]Department of Biomedical Laboratory Science, Namseoul University, Cheonan 330-707, Korea
Correspondence and requests for materials should be addressed to S. N. Park (suenie@kfda.or.kr)

Accepted 19 January 2009

Abstract

Acetaminophen (APAP) overdose is known to cause severe hepatotoxicity mainly through the depletion of glutathione. In this study, we compared the cytotoxic effects of APAP on both a normal murine hepatic cell line, BNL CL.2, and its SV40-transformed cell line, BNL SV A.8. Gene expression profiles for APAP-treated cells were also obtained using microarray and analyzed to identify differences in genes or profiles that may explain the differences of susceptibility to APAP in these cell lines. These two cell lines exhibited different susceptibilities to APAP (0-5,000 μM); BNL SV A.8 cells were more susceptible to APAP treatment compared to BNL CL.2 cells. A dose of 625 μM APAP, which produced significant differences in cytotoxicity in these cell lines, was tested. Microarray analysis was performed to identify significant differentially expressed genes (DEGs) irrespective of APAP treatment. Genes up-regulated in BNL SV A.8 cells were associated with immune response, defense response, and apoptosis, while down-regulated genes were associated with catalytic activity, cell adhesion and the cytochrome P450 family. Consistent with the cytotoxicity data, no significant DEGs were found in BNL CL.2 cells after treatment with 625 μM APAP, while cell cycle arrest and apoptosis-related genes were up-regulated in BNL SV A.8 cells. Based on the significant fold-changes in their expression, 8 genes were selected and their expressions were confirmed by quantitative real-time RT-PCR; there was a high correlation between them. These results suggest that gene expression profiles may provide a useful method for evaluating drug sensitivity of cell lines and eliciting the underlying molecular mechanism. We further compared the genes identified from our current *in vitro* studies to the genes previously identified in our lab as regulated by APAP in both C57BL/6 and ICR mice *in vivo*. We found that a few genes are regulated in a similar pattern both *in vivo* and *in vitro*. These genes might be useful to develop as *in vitro* biomarkers for predicting *in vivo* hepatotoxicity. Based on our results, we suggest that gene expression profiles may provide useful information for elucidating the underlying molecular mechanisms of drug susceptibility and for evaluating drug sensitivity *in vitro* for extrapolation to *in vivo*.

Keywords: Mouse genome microarray, Hepatotoxicity, Drug sensitivity, Gene expression, Real-time RT-PCR, Acetaminophen

An overdose of acetaminophen (APAP) can induce severe hepatotoxicity in experimental animals and in humans[1], although it is a safe and effective analgesic when used at therapeutic levels. The lethal toxicity resulting from APAP overdosing in human is well documented and is currently a matter of significant health concern. APAP is metabolized by cytochrome P-450 isoforms to the highly reactive metabolite *N*-acetyl-*p*-benzoquinoneimine (NAPQI), which at therapeutic APAP doses is detoxified by conjugation with glutathione[2]. However, at toxic doses of APAP, glutathione is depleted and NAPQI covalently binds to cysteine residues on proteins resulting in mitochondrial damage[3]. APAP-induced toxicity is associated with the cell death pathways[4], protein arylation[5], oxidative stress[6] and mitochondria homeostasis[7].

Toxicological and pharmacological studies designed to assess the safety and efficacy of new drugs and chemicals in the human population rely heavily on extrapolation from animal models. However, predicting the safety of drugs in the preclinical stage, prior to human testing, is one of the major bottlenecks in drug development. Recent advances in genome-scale sequencing have enabled the development of methods for quantitatively comparing the expression levels of all potentially expressed genes between different biological samples[8]. The application of such technology to toxicology, known as toxicogenomics, has the potential to identify a set of genes from a database of reference profiles; this gene set may be predictive of a compound's toxicity, identify its mechanisms of action, and permit extrapolation of its effects from one species to another[9]. This technique has been used increasingly as a means to evaluate and compare the *in vivo* and *in vitro* models commonly used for toxicological studies. Recently, we reported potential biomarkers of genotoxicity and carcinogenicity of chemicals with microarray gene expression profiling[10-14]. Several laboratories have recently reported gene expression profiling studies with APAP either for identifying the genomic toxicity markers or for elucidating the APAP toxicity mechanisms[15-17]. Several published reports have indicated oxidative stress as one of the possible mechanisms for APAP-induced hepatotoxicity[6,18,19]. In particular, Heinloth *et al.* (2004) found that altered gene expression patterns were suggestive of mitochondrial dysfunction and oxidative stress. In our previous studies, we found that APAP treatments in both C57BL /6 and ICR mice resulted in differential expressions of genes in the category of cell cycle arrest[17]. These include pathways related to cell cycle, MAPK signaling, calcium ion signaling, apoptosis, cellular metabolism, steroid synthesis, cysteine metabolism, porphyrin metabolism, glutathione metabolism and the urea cycle. These findings confirmed that the toxicity of APAP could result from induction of oxidative stress and apoptosis[17].

In transformed hepatic cells (BNL SV A.8), antioxidant enzyme activities were lower than in normal hepatic cells (BNL CL.2)[6]. Actually, important differences in the mRNA levels of several genes associated with the oxidative stress response were also found between normal BNL CL.2 and the SV40-transformed hepatic cell line, BNL SV A.8[20]. Thus, we hypo-

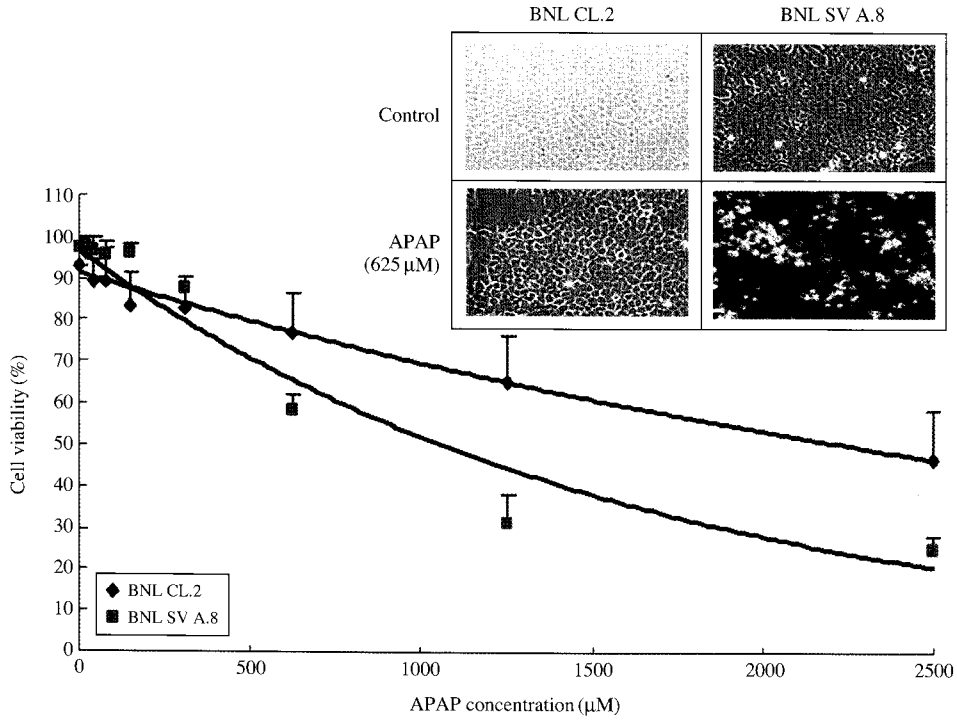

Figure 1. Effect of acetaminophen (APAP) on BNL CL.2 and BNL SV A.8 cells. The cells were treated with increasing concentrations of APAP ranging from 0 to 2,500 μM and then incubated in 96-well plates for 24 hrs before the addition of the cell proliferation reagent MTS. After an additional 2-h incubation, the absorbance was measured in an ELISA reader. The absorbance at 490 nm is expressed as the mean ± SD of triplicate determinants from one of three representative experiments. For comparison of two cell lines, the absorbance of the untreated group was defined as 100%. The inset shows representative morphology of the two cell lines after treatment with 625 μM APAP.

thesized that APAP may be able to induce growth inhibition of transformed cells more efficiently than in the normal counterpart since the oxidative stress level is higher in transformed cells; this higher oxidative stress level mimics drug-induced liver injury and may result in a more vulnerable status to APAP insult. In order to confirm this hypothesis, we investigated the susceptibility to APAP of the embryonic normal hepatic cell line (BNL CL.2) and its counter part, the SV40-transformed cell line (BNL SV A.8). We found that BNL SV A.8 is more sensitive to APAP. We also investigated and compared the global changes in gene expression resulting from treatment with APAP through microarray analysis in these two cell lines. Microarray analysis showed that the gene expression profiles differed between normal and transformed cells. Genes differentially expressed in the two cell lines were associated mainly with immune response, defense response, JAK-STAT signaling, apoptosis, catalytic activity, cellular metabolism, cell adhesion, and the cytochrome P-450 family for detoxification. These differentially expressed genes may be responsible for the sensitivity of BNL SV A.8 cells to APAP.

Cytotoxicity of APAP in Normal and Transformed Hepatic Cells, BNL CL.2 and BNL SV A.8

The concentrations of acetaminophen used for the microarray analysis were established in dose range-finding tests to evaluate the cytotoxicity in the normal hepatic cell line, BNL CL.2, and its SV40-transformed cell line, BNL SV A.8. There are significant morphological differences between normal and transformed cells (Figure 1, inset). BNL CL.2 cells form clusters with adjacent cells; however, in BNL SV A.8 cells, a subpopulation of smaller densely packed cells forms a second layer on top of the attached monolayer. For cytotoxicity assays, cells from these two cell lines were grown on 96-well plates and viable cell numbers were quantified using the MTS assay. Viabil-

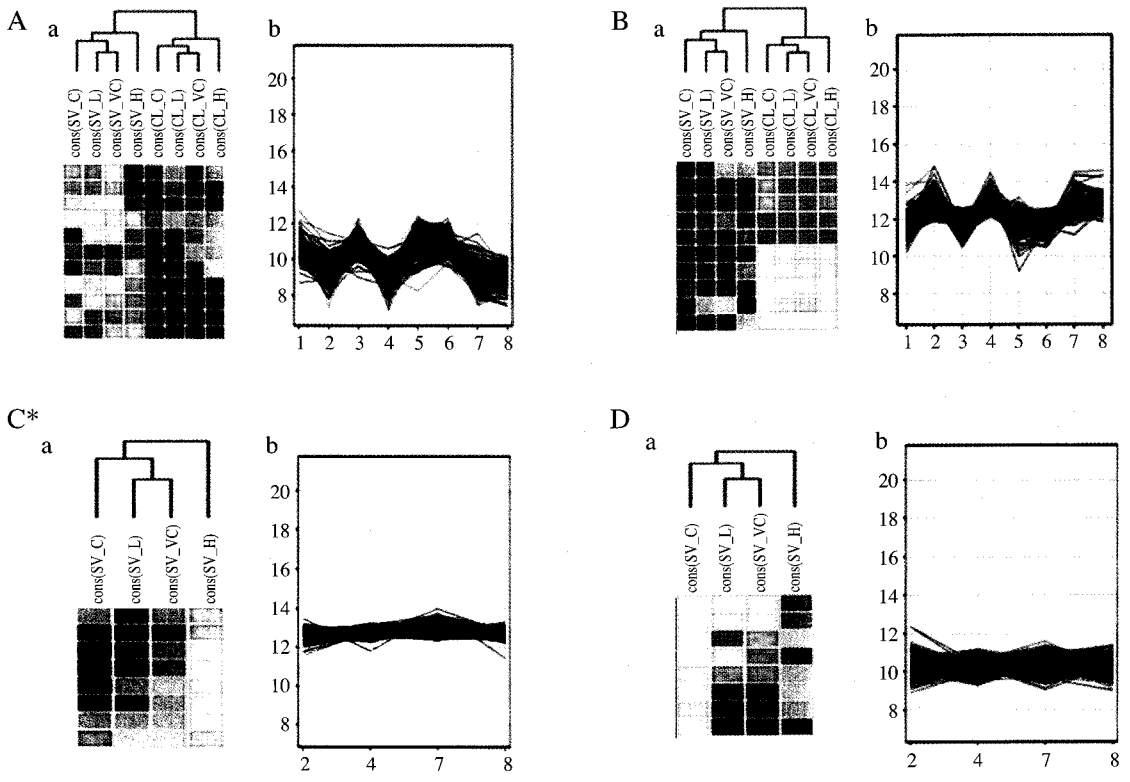

Figure 2. Hierarchical and K-means clustering of expressed genes in BNL CL.2 and BNL SV A.8. A & B : up- and down-regulated genes in BNL SV A.8 compared to BNL CL.2, a : hierarchical clustering, b : K-means clustering, respectively. C* & D : up- and down-regulated genes in 625 μM APAP-treated group compared to untreated group in BNL SV A.8, respectively. In K-means clustering, green lines indicate all of the clustered genes and blue lines show significant genes among them. Cons : mean of raw data from three independent experiments, SV : BNL SV A. 8, CL : BNL CL.2, C : control, VC : vehicle control, L : 62.5 μM APAP, H : 625 μM APAP, 1 : SV_C, 2 : CL_C, 3 : SV_L, 4 : CL_L, 5 : SV_H, 6 : SV_VC, 7 : CL_H, 8 : CL_VC. Expressed genes in BNL CL.2 and BNL SV A.8 were clustered by AVADIS. In the clustering, the two cell lines were nicely separated as shown in A & B. In C* & D, only in 625 μM APAP-treated group in BNL SV A.8 cells did up- or down-regulated genes appear.

ity curves of the two cell lines *in vitro*, which were generated following exposure to APAP, demonstrated that the IC_{50} of APAP was approximately 2,000 and 1,000 μM in BNL CL.2 and BNL SV A.8 cells, respectively (Figure 1). In particular, 625 μM APAP caused more than 40% decrease in the cell viability of BNL SV A.8 cells while resulting in less growth inhibition (20%) in BNL CL.2 cells. These results confirmed that transformed BNL SV A.8 cells are more sensitive than BNL CL.2 cells to APAP-mediated cytotoxicity.

Microarray Analysis of Gene Expression Patterns in BNL CL.2 and BNL SV A.8 Cells

Microarray analysis was performed in three independent experiments to assure reproducibility. Scatter plot showed that the correlation coefficient of the triplicate hybridizations was more than 0.96 after normalization (data not shown). The microarray results obtained from three independent hybridizations for BNL SV A.8 cells were averaged and expressed as the fold-change from BNL CL.2 cells. The results were compared to identify similarities and differences in the gene expression profiles. Microarray data corresponding to BNL SV A.8 cells were compared to the microarray data from BNL CL.2 cells using *t*-test, and a specific gene was considered significantly and differentially expressed if the two-tailed *t*-test *P*-value was less than 0.05 and the fold-change was greater than 3. Based on these two criteria, there were 739 genes that were differentially expressed in the two APAP-untreated cell lines (data not shown).

In order to classify the genes into groups with a similar pattern of expression and to identify genes exhibiting differential expression between BNL CL.2 and BNL SV A.8 cells, K-means clustering was performed using the 11,699 filtered genes with signal-to-noise ratio (S/N) >3 and the flag value below 5,000. From 30 distinct clusters of gene expression patterns obtained in the analysis, differentially expressed genes with significance between the two cells lines were demonstrated (Figure 2). Among the genes in the six clusters identified from clustering analysis, genes showing greater than 3-fold increase or decrease in expression level in BNL SV A.8 compared to BNL CL.2 cells are listed in Table 2 and Table 3, respectively. These genes are classified by their functional properties. The genes up-regulated in BNL SV A.8 cells belong to the categories of immune response, defense response, JAK-STAT signaling, and apoptosis (Table 2). Meanwhile genes in the categories of catalytic activity, cellular metabolism, cell adhesion and cytochrome P-450 family for detoxification were down-regulated (Table 3). According to BIOCARTA, these genes are likely to be involved in pathways related to the nuclear receptor in lipid metabolism, toxicity, and multi-drug resistance factors.

Microarray Analysis of Gene Expression Patterns in BNL CL.2 and BNL SV A.8 Cells after APAP Treatment

For comparison of gene expression profiles after APAP treatment, 0 (vehicle control), 62.5 and 625 μM APAP were tested. A single time point of 24 h after the treatment was chosen for cell harvesting to eliminate the potentially confusing contribution of nonspecific immediate early stress responses in cells exposed to APAP. Average fold-change was calculated from three independent experiments with samples at 24 h after APAP treatment in BNL CL.2 and BNL SV A.8 cells. There were 79 and 78 genes that were differentially expressed genes in BNL CL.2 cells after treatment with 62.5 and 625 μM APAP compared to vehicle control, respectively (data not shown). There were 58 and 126 genes that were differentially expressed in BNL SV A.8 cells after treatment with 62.5 and 625 μM APAP compared to vehicle control, respectively (data not shown).

Differentially expressed genes obtained from 625 μM APAP-treated BNL CL.2 and BNL SV A.8 cells were further analyzed since this concentration resulted in the greatest differences in cytotoxicity and also in a large number of differentially expressed genes in the two cell lines (78 vs. 126) for practical comparison. Clustering methods were used to group genes with similar patterns of expression and to identify genes exhibiting differential expression in BNL SV A.8 cells and BNL CL.2 cells in response to APAP. K-means clustering was performed using the 11,699 filtered genes with signal-to-noise ratios (S/N) >3 and the flag value below 5,000. From 30 distinct clusters of gene expression patterns obtained in the analysis, significantly up-regulated and down-regulated clusters were demonstrated in response to 625 μM APAP, specific for BNL SV A.8 cells (Figure 2). But no significant cluster groups were found in BNL SV A.8 cells after treatment with 62.5 μM APAP. Among the genes in those identified clusters, genes showing a ≥ 3-fold change in expression level from control were selected for further analysis and classification by their functional properties. The number of up- and down-regulated genes in BNL CL.2 cells and BNL SV A.8 cells after treatment with 625 μM APAP was 8 and 50, respectively (Figure 3). The genes up-regulated in BNL SV A.8 cells with 625 μM APAP treatment belong to the categories of cell cycle arrest and MAP kinase pathway while the genes in the categories of anti-inflammatory, catalytic activity, and cell differ-

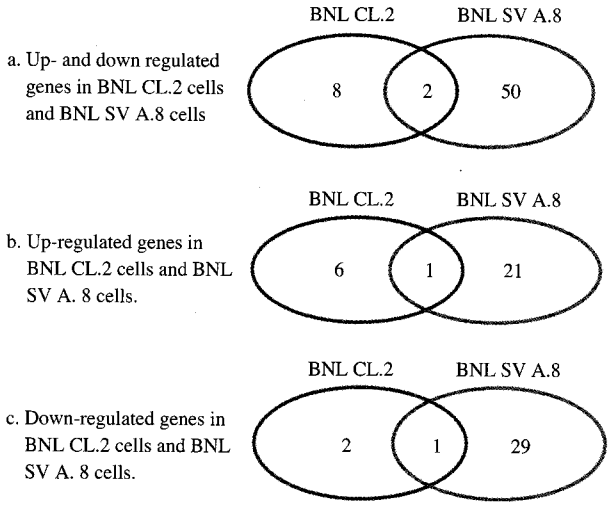

Figure 3. Differentially expressed genes in BNL CL.2 cells and BNL SV A.8 cells after treatment with 625 μM APAP. Among the genes in K-means clusters, there are genes showing greater than 3-fold increase or decrease in expression level and $P<0.05$ in BNL CL.2 cells or BNL SV A.8 cells compared to vehicle control. Total numbers of up- and down-regulated genes were 10 and 52 for BNL CL.2 cells and BNL SV A.8 cells, respectively, after APAP treatment. Venn diagrams of these genes were drawn, and 8 and 50 genes were unique to each cell line (Figure 3a), while 6 and 21 up-regulated and 2 and 29 down-regulated genes were unique to each cell line, respectively (Figure 3b and 3c).

entiation were down-regulated (Table 4).

However, no significant cluster groups were found in BNL CL.2 cells after treatment with APAP, even at 625 μM APAP; BNL CL.2 cells exhibit less overt cytotoxic effects, suggesting a functional difference in response to APAP in normal and transformed hepatic cells (data not shown).

Analysis of The Expression of The Selected Genes by Quantitative Real-Time RT-PCR

Real-time RT-PCR was performed on the eight genes described in Table 1 in an attempt to confirm the significant changes in expression of the genes selected in the microarray analysis. These genes were selected based on their distinct expression level changes: up- or down-regulated in BNL SV A.8 cells compared to BNL CL.2 cells (Table 2, 3) and in 625 μM APAP-treated groups compared to vehicle control group in BNL SV A.8 cells (Table 4). These genes included chemokine ligand 17 (*Ccl17*), suppressor of cytokine signaling 2 (*Socs2*), an unknown function protein (*D12Ertd647e*), junction adhesion molecule 4 (*Jam4*), annexin 10 (*Anxa10*), cyclin-dependent kinase inhibitor 1a (*Cdkn1a*), sestrin (*Sesn2*), and dual specificity phosphatase 1 (*Dusp1*). Glyceraldehyde-3-phosphate

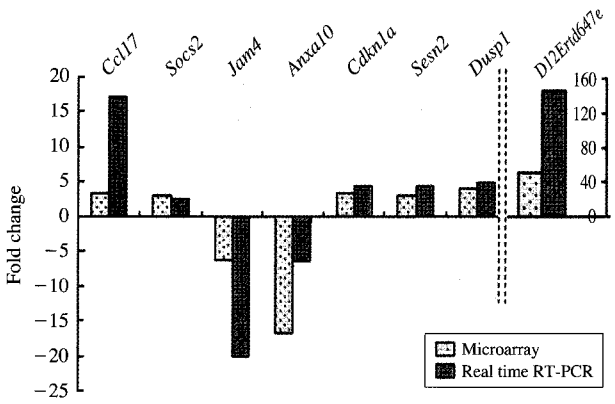

Figure 4. Quantitative real-time RT-PCR analysis of selected genes compared with microarray results. The expression of selected genes was measured by real-time RT-PCR. Shown are mean expression ratios obtained by either microarray or RT-PCR analysis. *Ccl17, Socs2*; and *D12Ertd647e, Jam4, Anxa10* genes differentially expressed in BNL SV A.8 cells compared to BNL CL.2 cells. *Cdkn1a, Sesn2* and *Dusp1*; genes differentially expressed in 625 μM APAP-treated groups compared to vehicle control group in BNL SV A.8 cells.

Table 1. Primers used for confirmation of selected gene expression changes in real-time RT-PCR.

Gene symbol	GenBank accession no.	Assay ID	Product size (bp)
Ccl17	BC028505	MM00516136_M1	76
Socs2	AK048608	MM00850544_G1	137
D12Ertd647e	AK003665	MM01329985_M1	58
Jam4	AF537215	MM00511211_M1	82
Anxa10	AK020288	MM00507886_M1	73
Cdkn1a	AK007630	MM00432448_M1	96
Sesn2	BC005672	MM00460679_M1	58
Dusp1	BC006967	MM00457274_G1	65

dehydrogenase (*Gapdh*) was used as a reference gene; its expression levels were similar to those observed for the genes of interest and it was constitutively expressed across all groups. Prior to use for confirmation studies, primer sets (Table 1) synthesized for these genes were evaluated to ensure that the working efficiencies of the primers designed for the target and the reference genes were approximately equal and were appropriate for use (data not shown).

For all eight genes tested by RT-PCR for confirmation studies, there was good correlation between the quantitative real-time RT-PCR data and the microarray data (Figure 4). Specifically, *D12Ertd647e*, which showed high level of expression in the microarray experiment (50.6-fold), also demonstrated comparable expression in the real-time RT-PCR assays (146.6-fold). However, *Ccl17* showed a much higher level of ex-

Table 2. Genes significantly up-regulated in BNL SV A.8 cells compared to BNL CL.2 cells.

Related pathway	Gene symbol	GenBank accession no.	Gene name	Gene function	Fold change
Immune response	*Peli1*	BC016515	pellino 1	IL-1 mediated signaling activity	3.0
	Tspyl4	BC030922	tspy-like 4	macromolecule metabolism	4.0
	Ltk	BC055898	leukocyte tyrosine kinase	ATP binding, protein kinase activity	3.9
	Agc1	L07049	aggrecan 1	macromolecular biosynthesis	8.6
Defense response	*Ccl17*	BC028505	chemokine (c-c motif) ligand 17	response to stress	3.2
	Pros1	L27439	proteins (alpha)	EGF-like, type 3, response to stress	3.7
JAK-STAT signaling pathway	*Socs2*	AK048608	suppressor of cytokine signaling 2	negative regulation of cellular process	3.0
Apoptosis	*Proc*	BC013896	protein c	apoptosis, cell death	3.4
Growth	*Hoxb13*	AK077273	homeo box b13	development and growth	5.8
	Grb7	BC003295	growth factor receptor bound protein 7	Ras-associating intracellular signaling	3.2
	Fndc4	BC027164	fibronectin type iii domain containing 4	fibronectin	11.1
	Tmeff2	BC034850	transmembrane protein with egf-like and two follistatin-like domains 2	growth factor activity	5.0
Unknown	*D12Ertd647e*	AK003665	dna segment, chr 12, erato doi 647, expressed	unknown	50.6
	C130038G02Rik	BC055016	riken cdna c130038g02 gene	unknown	6.3

Table 3. Genes significantly down-regulated in BNL SV A.8 cells compared to BNL CL.2 cells.

Related pathway	Gene symbol	GenBank accession no.	Gene name	Gene function	Fold change
Catalytic activity	*Ephx2*	BC015087	epoxide hydrolase 2. cytoplasmic	epoxide hydrolase activity	−8.7
Cellular metabolism	*Stra6*	AF062476	stimulated by retinoic acid gene 6	integral to membrane	−5.8
	Htr1b	Z11597	5-hydroxytryptamine receptor 1b	cell communication	−6.8
	Aox1	BC026132	aldehyde oxidase1	iron ion bonding	−4.2
	Fxyd3	BC051033	fxyd domain-containing ion transport regulator 3	ion channel activity	−14.6
	Dcn	BC060126	decorin	proteoglycan	−3.9
Cell adhesion	*Jam4*	AF537215	junction adhesion molecule 4	cell-cell adhesion	−6.2
Cytochrome P-450 family for detoxification	*Anxa10*	AK020288	annexin A10	anti-inflammatory	−16.7
	P2ry2	L14751	purinergic receptor P2Y, G-protein coupled 2	G-protein coupled receptor activity	−8.0

pression in the RT-PCR assay (17.1-fold) compared to the microarray analysis (3.2-fold).

Discussion

The hepatotoxicity of APAP sometimes leads to acute liver failure[21] despite its analgesic and antipyretic properties. The metabolic activation of APAP that leads to glutathione depletion is known to be an important step in APAP-induced liver toxicity[22,23]. The depletion of cellular glutathione, a natural antioxidant, leaves the cell particularly vulnerable to oxidative insults following APAP overdose[6]. The present study demonstrated that the SV40-transformed BNL SV A.8 hepatic cell line, in which the anti-oxidant en-

Table 4. Genes significantly changed after treatment with 625 μM APAP in BNL SV A.8 cells.

Related pathway	Gene symbol	GenBank accession no.	Gene name	Gene function	Average fold change	
					Vehicle vs. 62.5 μM APAP	Vehicle vs. 625 μM APAP
Up-regulated genes						
Cell cycle arrest	*Cdkn1a*	AK007630	cyclin-dependent kinase inhibitor 1a (p21)	cell cycle arrest	1.0	3.4
	Sesn2	BC005672	PA26 p53-induced protein (sestrin)	cell cycle arrest	−1.0	3.0
MAP kinase pathway	*Dusp1*	BC006967	dual specificity phosphatase 1	regulation of MAP Kinase Pathways Through Dual Specificity Phosphatases	1.3	3.9
Apoptosis	*Il18*	D49949	interleukin 18	apoptosis, immune cell synthesis	1.3	4.5
	Gdf15	BC067248	growth differentiation factor 15	transforming growth factor beta	−1.0	6.4
Down-regulated genes						
Anti-inflammatory	*Anxa13*	AJ306451	annexin a13	anti-inflammatory, anticoagulant protein	−1.1	−4.4
Catalytic activity	*Sult1c2*	BC022665	sulfotransferase family, cytosolic, 1C, member 1	catalytic activity, sulfotransferase activity	−1.2	−5.5
Cell differentiation	*Sprr2a*	AY158986	small proline-rich protein 2a	cellular morphogenesis	−1.3	−19.2
	Sprr2b	AY158987	small proline-rich protein 2b	cell differentiation, ectoderm development	−1.4	−25.3

zyme activities are lower than in the normal hepatic cell line counterpart BNL CL.2[6], was more sensitive to APAP-mediated cytotoxicity than the normal cell line was. Furthermore, oligonucleotide microarray analyses were performed, not only to compare the basal expression in the normal hepatic cell line to that in the transformed cell line, but also to identify genes responsive to APAP treatment in the two cell lines in order to better understand the underlying mechanisms of hepatotoxicity and cytotoxicity of APAP. We utilized the microarray platform from Applied Biosystems since Wang *et al.* (2006) validated that this microarray platform has acceptable sensitivity and accuracy in detecting differential expression, especially for genes with high and medium expression levels and for detecting >2-fold changes. Also, excellent fold-change correlation is obtained with other microarray platform data despite the identification of inter-platform discordance in lists of genes measured as differentially expressed[24].

Three independent hybridization experiments were performed to identify differentially expressed genes. Genes were considered differentially expressed when average expression levels were more than three-fold different and when *P*-values were lower than 0.05. Not surprisingly, there is considerable variability in basal gene expression between the normal hepatic cell line, BNL CL.2, and its transformed cell line, BNL SV A.8.

These two cell lines had differences in the basal expression of 739 genes. K-means clustering also identified differences between normal and transformed cells in the expression of genes in several functional categories. The microarray data identified that the genes in the category of immune response, defense response, and apoptosis were significantly more expressed in BNL SV A.8 cells compared to BNL CL.2 cells. Also, the genes involved in catalytic activity, cellular metabolism, cell adhesion, and cytochrome P-450 family for detoxification were significantly down-regulated in BNL SV A.8 cells. Among the up-regulated or down-regulated genes identified by clustering analysis (Figure 2), genes showing greater than 3-fold change in expression level are presented in Tables 2 and 3, respectively. For instance *Ccl17* (chemokine ligand 17), *Socs2* (suppressor of cytokine signaling 2), *Grb7* (growth factor receptor bound protein 7), and *D12Ertd647e* (unknown protein) were expressed at significantly higher levels in the transformed cell line than in the normal cell line, suggesting that

Table 5. Correlation of differentially expressed genes after treatment with APAP *in vivo* and *in vitro*.

Related pathway		Strain	Gene symbol	Gene name	Fold change
Cell cycle arrest	*In vivo*	C57BL/6	*Cdkn1a*	cyclin-dependent kinase inhibitor 1A (P21)	4.0
		ICR	*Cdkn1a*	cyclin-dependent kinase inhibitor 1A (P21)	17.5
	In vitro	BNL SV A.8	*Cdkn1a*	cyclin-dependent kinase inhibitor 1A (P21)	3.4
			Sesn2	PA26 p53-induced protein (sestrin)	3.0
MAP kinase pathway	*In vivo*	C57BL/6	*Gadd45g*	growth arrest and DNA-damage-inducible 45 gamma	3.7
		ICR	*Dusp8*	dual specificity phosphatase 8	12.4
	In vitro	BNL SV A.8	*Dusp1*	dual specificity phosphatase 1	3.9
Apoptosis	*In vivo*	C57BL/6	*Gadd45g*	growth arrest and DNA-damage-inducible 45 gamma	3.7
		ICR	*Gadd45a*	growth arrest and DNA-damage-inducible 45 alpha	39.6
			Gadd45b	growth arrest and DNA-damage-inducible 45 beta	12.2
			Casp4	caspase 4, apoptosis-related cysteine protease	8.0
			Myc	myelocytomatosis oncogene	20.2
	In vitro	BNL SV A.8	*Il18*	interleukin 18	4.5
			Gdf15	growth differentiation factor 15	6.4
Catalytic activity	*In vivo*	ICR	*Sult1c2*	sulfotransferase family, cytosolic, 1C, member 1	−3.9
	In vitro	BNL SV A.8	*Sult1c2*	sulfotransferase family, cytosolic, 1C, member 1	−5.5

their overexpression could be related to the transformed phenotype or the drug-sensitivity of the liver cells. Increased *Socs2* protein and mRNA expression has been associated with leukemia[25]. Overexpression of *Grb7* proteins may contribute to the invasive potential of cancer cells[26]. *D12Ertd647e*, which is dramatically up-regulated, is presumed to encode a protein involved in response to stress, but there is no evidence available to link it to tumor growth or APAP-sensitivity yet. In contrast, the expression of 9 genes, including *Htr1b, Aox1, Fxyd3* and *Anxa10*, was significantly decreased in the transformed cell line compared to the normal cell line. *Htr1b*, which encodes the serotonin1B receptor, is a candidate gene for alcohol and drug sensitivity[27]. *Aox1*, aldehyde oxidase 1[28], may be involved in oxygen tolerance such as the action of superoxide dismutase 1. Regulation of *Fxyd3* which regulates chloride transport and Na^+/K^+ATPase is associated with the drug-resistance period[29]. Safaei *et al.* (2005) reported a significant increase in *Anxa10* expression in drug-resistant human ovarian carcinoma cells, implying its role in acquired drug resistance. The down-regulation of *Anxa10* (annexin A10) is also associated with malignant phenotype of hepatocytes and vascular invasion[30].

We identified APAP-induced differences in the gene expression in the two cell lines. In BNL CL.2 cells, 79 and 78 genes were differentially expressed at 62.5 and 625 μM APAP, respectively (data not shown). In BNL SV A.8 cells, 58 and 126 genes were differentially regulated after treatment with 62.5 and 625 μM APAP, respectively (data not shown). From up-regulated and down-regulated gene clusters showing differential gene regulation in response to 625 μM APAP that were specific for BNL SV A.8 cells, genes showing more than 3-fold change in expression versus vehicle control were selected (Table 4). *Dusp1* and *Gdf15* expressions were increased about 3.9- and 6.4-fold ($P<0.05$) with 625 μM APAP in BNL SV A.8 cells, respectively. The induction of *Dusp1* (dual spe-

cificity phosphatase 1) is reported to play an important regulatory role in the human cellular response to environmental stress[31]. *Gdf15*, which is one of the divergent members of the TGF-β superfamily, is induced in hepatocytes by surgical and chemical injury[32]. In contrast, APAP exposure significantly decreased *Sprr2a* and *Sprr2b* expressions (19.2-fold and 25.3-fold with 625 μM APAP treatment, respectively). These two gene products, which are structural components of the cornified cell envelope, are primarily associated with cell differentiation and morphogenesis[33].

To validate the microarray data, eight genes (Table 1) that exhibited significant differences in expression level as shown in Tables 2, 3 and 4 were selected for quantitative real-time PCR analyses. Although the expression change of all eight genes detected by real-time RT-PCR generally showed the same trend as in the microarray, the extent of change detected by the two methods varied (Figure 4). One notable example of such a discrepancy between real-time RT-PCR and microarray results is the expression of the *Ccl7* gene (17.1-fold vs. 3.2-fold up-regulation, respectively), which has an important role in the development of pulmonary fibrosis via recruitment of lymphocytes and macrophages[34]. The extent of expression for *Socs2* and *D12Ertd647e* was similar for both microarray analysis and real-time RT-PCR. *Socs2* (suppressor of cytokine signaling-2) is a regulator of growth hormone signal transduction[35]. The marked up-regulation of the *D12Ertd647e* in BNL SV A.8 cells was confirmed by real-time RT-PCR. In fact, the PCR product of *D12Ertd647e* was barely detectable in BNL CL.2 cells while its expression was greatly increased in BNL SV A.8 cells, implying that this gene would be a good candidate biomarker for cell transformation or drug sensitivity. Although *D12Ertd647e* is identified only by its DNA sequence and its function is still unknown, it can be considered 'signatory' for the outcome since the alteration of its expression is highly correlated with a given treatment. Further experiments are needed to validate and to understand the role of *D12Ertd647e* mRNA levels in APAP treatment. The level of down-regulation determined for *Jam4* and *Anxa10* by the two methods in BNL SV A.8 cells was also quite different. For instance, *Jam4* (junction adhesion molecule 4), which provides adhesion machinery at tight junctions[36], showed a much higher level of down-regulation in real-time RT-PCR (-20.2-fold) than in the microarray data (-6.2-fold). These discrepancies may be caused by differences in the sensitivity and dynamic range of the methodologies used to determine gene expression and in the specificity of the primer/probe set. Still, we cannot exclude the possibility that fold-change values obtained from microarray analysis can be particularly misleading in cases where low or no hybridization signals are detected in one of the samples, although this seems not to be the case in our experiments.

The data from this study imply that gene-expression profiling could reveal the mechanisms of action of chemicals and drugs. However, the current methods used for monitoring differential gene expression exclude the direct detection of changes in genes whose regulation probably does not occur at the transcriptional level[37]. The vast majority of the mouse genome appears to be unresponsive to chemical stress[38]. In fact, APAP has been known to initiate its toxicity by the cytochrome P450-catalyzed activation of acetaminophen to an electrophilic intermediate[22] and not by direct induction of gene expression. Despite these limitations, our study identified several genes and functional clusters that may help discriminate the difference of sensitivity to APAP in the two cell lines, suggesting that microarray analysis may constitute a useful method for evaluating drug sensitivity. Previously we also studied APAP effects in both C57BL/6 and ICR mice *in vivo*[17,39]: some of the differentially expressed genes were associated with cell cycle arrest, MAP kinase pathway, apoptosis, and catalytic activity, as in BNL SV A.8 cells *in vitro* (Table 5). We found that a few genes of similar function were regulated in a similar pattern *in vivo* and *in vitro*. In particular, *Cdkn1a*, cyclin-dependent kinase inhibitor 1A gene, and *Sult1c2*, sulfotransferase family, cytosolic, 1C, member 1 gene, were up-regulated consistently both *in vivo* (C57BL/6 and ICR mice) and *in vitro* (BNL SV A.8) after treatment with APAP, suggesting that they could function as signatory genes for APAP toxicity.

However, further investigation is required to interpret the specific functional significance of these changes in gene expression and to assess their value as biomarkers of hepatotoxicity *in vivo* or of drug-sensitivity *in vitro* and *in vivo*.

Materials & Methods

Materials

Dulbecco's modified Eagle's medium (DMEM), fetal bovine serum (FBS) and penicillin-streptomycin were purchased from Invitrogen (Carlsbad, CA). CellTiter 96 Aqueous Non-Radioactive Cell Proliferation Assay kit was obtained from Promega Co. (Madison, WI), while the cytotoxicity detection kit was from Roche Molecular Biochemicals (Indianapolis, IN). Mouse Genome Survey Microarray gene chips were supplied by Applied Biosystems (Foster City, CA).

This microarray platform has 33,012 probes, which are 60-mers and lie mostly within 1,500 base pairs of the 3′-end of the source transcript. APAP was obtained from Sigma (St. Louis, MO).

Cell Lines, Cell Culture and Chemical Treatments

Murine embryonic normal hepatic cell line, BNL CL.2 cells (ATCC TIB-73), and its SV40-transformed cell line, BNL SV A.8 cells (ATCC TIB-74), were from American Type Culture Collection (ATCC, Manassas, VA). The cells were cultured in DMEM supplemented with 100 units of penicillin-streptomycin/mL, 2 mM L-glutamine, and 10% FBS at 37°C in a 5% CO_2 atmosphere. Acetaminophen was dissolved in dimethyl sulfoxide (DMSO) and was freshly diluted in culture media for each experiment. Vehicle concentrations were less than 0.5% in all experiments. After 24 h of treatment, cells were harvested for RNA extraction.

Cytotoxicity Assay Using MTS Method

The inhibition of cell proliferation was assessed using the MTS [3-(4,5-dimethylthiazol-2-yl)-5-(3-carboxymethoxyphenyl)-2-(4-sulfophenyl)-2H-tetrazolium, inner salt] assay, conducted with the CellTiter 96 Aqueous Non-Radioactive Cell Proliferation Assay kit. Briefly, cells were sub-cultured on a 96-well plate with 2.5×10^4 cells/well in 50 μL of medium. After 24-h incubation, the medium in the 96-well plate was discarded and replaced with medium containing different concentrations of APAP (20, 40, 79, 157, 313, 625, 1,250, and 2,500 μM) or 0.5% DMSO (vehicle control). The treated cells were incubated at 37°C for 24 h, each well then received 20 μL of MTS test solution prepared by mixing 2 mL of MTS-labeling reagent and 100 μL of electron coupling reagent (PMS: phenazine methosulfate). After 2-h incubation, the absorbance of the sample was measured with an ELISA reader (Bio-Rad Laboratories, Hercules, CA) at a test wavelength of 490 nm. The IC_{50} value of APAP, the concentration which gives 50% decrement of cell viability, was calculated.

RNA Isolation and Microarray Gene Expression Profiling

Total RNAs were extracted using the RNeasy Mini kit (Qiagen, Valencia, CA). The yield of RNA was determined spectrophotometrically by measuring the optical density at 260 nm. The quality of RNA was evaluated using the Agilent 2100 Bioanalyzer (Agilent Technologies, Palo Alto, CA). Total RNA was converted into double-stranded cDNA using a Chemiluminescent RT-IVT labeling Kit (Applied Biosystems) and an oligo$(dT)_{24}$ primer. Digoxigenin-labeled cRNA was generated from the double-stranded cDNA using the Chemiluminescent RT-IVT labeling kit. Labeled cRNA was purified using a cRNA purification kit (Applied Biosystems) and analyzed for quality and quantity using spectrometry and the Agilent 2100 Bioanalyzer. Each cRNA sample was fragmented by incubation in fragmentation buffer for 30 min at 60°C. The Mouse Genome Survey Microarray gene chip (Applied Biosystems) was hybridized with the fragmented digoxigenin-labeled cRNAs at 55°C for 16 h and then washed. After the washing procedure, chemiluminescent detection, image acquisition and analysis were performed using the Chemiluminescent Detection Kit and Applied Biosystems 1700 Chemiluminescent Microarray Analyzer according to the manufacturer's protocols. The chemiluminescent signals from the scanned images were quantified, corrected for background, and spot- and spatially-normalized using the 1700 Chemiluminescent Microarray Analyzer (Applied Biosystems). Three independent microarray analyses were performed for each RNA sample from three independent experiments.

Data Analysis

Gene expression data from microarray were input to AVADIS (Strand Life Sciences, Redwood city, CA). The signal log ratio values, which represent ratios of hybridization signals between BNL CL.2 and BNL SV A.8 or between vehicle- and APAP-treated cells, were calculated after quantile normalization. A signal log ratio of 1 represents a gene that shows a 2-fold increase in expression. The genes with the signal-to-noise (S/N) of the log ratios threshold (more than 3) were filtered. Also, if the flag value of a probe was above 5000, the signal value of the probe was considered a missing value and was replaced with NA. Fold-changes were calculated between BNL CL.2 and BNL SV A.8 cells and between vehicle- and APAP-treated cells. K-means clustering was performed to identify genes that have a similar differential expression profile across conditions. Pathway analyses were conducted using DAVID (The Database for Annotation, Visualization and Integrated Discovery) (http://david.abcc.ncifcrf.gov/) and PANTHER (Protein ANalysis THrough Evolutionary Relationships) (http://www.pantherdb.org/).

TaqMan RT-PCR Analysis

Selected genes showing expression differences in the microarray analyses were further confirmed by quantitative real-time RT-PCR. Total RNAs were converted to cDNAs using TaqMan Reverse Transcription reagents (Applied Biosystems). Quantitative RT-PCR was performed with the use of TaqMan univer-

sal master mix; TaqMan probes and primers were Assay-on-Demand gene Expression products (Applied Biosystems). Gene-specific TaqMan probes used for the validation PCR are presented in Table 1 (primer sequences are not available from TaqMan). To control the integrity of RNA and the differences attributable to errors in experimental manipulation from tube to tube, primers for mouse glyceraldehyde-3-phosphate dehydrogenase (*Gapdh*), a housekeeping gene, were used in separate PCR reactions. PCR amplifications were performed with a 7500 Real-time PCR system (Applied Biosystems) using the following programs: (i) Uracil DNA glycosylase incubation (1 cycle: 50°C for 2 min); (ii) AmpliTaq Gold activation (1 cycle: 95°C for 10 min); (iii) amplification (50 cycles: 95°C for 15 s, 60°C for 60 s). A negative control reaction (the absence of template) was performed simultaneously in triplicate for each primer pair. Change in fluorescence levels of the FAM-labeled gene of interest was monitored at every cycle. The cycle (C_t) at which fluorescence was significantly above the background for each reaction was determined by Applied Biosystems Sequence Detection Software 1.9. Quantification was performed by comparing the fluorescence of PCR products of the selected genes with the fluorescence of the *Gapdh* gene product. Mean ± SD of triplicate C_t values for each gene of interest was calculated. The statistical analyses were performed using JMP software (SAS Institute, Cary, NC). Differences were regarded as statistically significant at the level of $P < 0.05$.

Acknowledgements

This work was supported by research grants, 06131-Omics_401 (2006) and 06131_Basic_629 (2006), to Dr. Sue Nie Park from the Korea Food and Drug Administration.

References

1. Sun, Y., Oberley, L. W., Elwell, J. H. & Sierra-Rivera, E. Antioxidant enzyme activities in normal and transformed mouse liver cells. *Int J Cancer* **44**:1028-1033 (1989).
2. Mitchell, J. R., Jollow, D. J., Potter, W. Z., Gillette, J. R. & Brodie, B. B. Acetaminophen-induced hepatic necrosis. IV. Protective role of glutathione. *J Pharmacol Exp Ther* **187**:211-217 (1973).
3. Pumford, N. R., Halmes, N. C. & Hinson, J. A. Covalent binding of xenobiotics to specific proteins in the liver. *Drug Metab Rev* **29**:39-57 (1997).
4. Ray, S. D. & Jena, N. A hepatotoxic dose of acetaminophen modulates expression of BCL-2, BCL-X (L), and BCL-X (S) during apoptotic and necrotic death of mouse liver cells *in vivo*. *Arch Toxicol* **73**:594-606 (2000).
5. Gibson, J. D., Pumford, N. R., Samokyszyn, V. M. & Hinson, J. A. Mechanism of acetaminophen-induced hepatotoxicity: covalent binding versus oxidative stress. *Chem Res Toxicol* **9**:580-585 (1996).
6. Adamson, G. M. & Harman, A.W. Oxidative stress in cultured hepatocytes exposed to acetaminophen. *Biochem Pharmacol* **45**:2289-2294 (1993).
7. Burcham, P. C. & Harman, A. W. Acetaminophen toxicity results in site-specific mitochondrial damage in isolated mouse hepatocytes. *J Biol Chem* **266**:5049-5054 (1991).
8. Brown, P. O. & Botstein, D. Exploring the new world of the genome with DNA microarrays. *Nat Genet* **21**: 33-37 (1999).
9. Young, R. R. Genetix toxicology: Web resources. *Toxicology* **173**:103-121 (2002).
10. Kim, J. H. *et al.* Toxicogenomics study on TK6 human lymphoblast cells treated with mitomycin C. *Mol Cell Toxicol* **3**:165-171 (2007).
11. Kim, J. Y. *et al.* Identification of potential biomarkers of genotoxicity and carcinogenicity in L5178Y mouse lymphoma cells by cDNA microarray analysis. *Environ Mol Mutagen* **45**:80-89 (2005).
12. Lee, E. M. *et al.* Genetic toxicity test of *o*-Nitrotoluene by ames, micronucleus, comet assays and microarray analysis. *Mol Cell Toxicol* **3**:107-112 (2007).
13. Lee, M. *et al.* cDNA microarray gene expression profiling of hydroxyurea, paclitaxel, and p-anisidine, genotoxic compounds with differing tumorigenicity results. *Environ Mol Mutagen* **42**:91-97 (2003).
14. Lee, W. S. *et al.* Genetic toxicity test of 8-hydroxyquinoline by ames, micronucleus, comet assays and microarray analysis. *Mol Cell Toxicol* **3**:90-97 (2007).
15. Heinloth, A. N. *et al.* Gene expression profiling of rat livers reveals indicators of potential adverse effects. *Toxicol Sci* **80**:193-202 (2004).
16. Reilly, T. P. *et al.* Expression profiling of acetaminophen liver toxicity in mice using microarray technology. *Biochem Biophys Res Commun* **282**: 321-328 (2001).
17. Suh, S. K. *et al.* Gene expression profiling of acetaminophen induced hepatotoxicity in mice. *Mol Cell Toxicol* **2**:246-243 (2006).
18. Arnaiz, S. L., Llesuy, S., Cutrin, J. C. & Boveris, A. Oxidative stress by acute acetaminophen administration in mouse liver. *Free Radic Biol Med* **19**:303-310 (1995).
19. Reid, A. B., Kurten, R. C., McCullough, S. S., Brock, R. W. & Hinson, J. A. Mechanisms of acetaminophen-induced hepatotoxicity: role of oxidative stress and mitochondrial permeability transition in freshly isolated mouse hepatocytes. *J Pharmacol Exp Ther* **312**: 509-516 (2005).
20. Vasiliou, V., Buetler, T., Eaton, D. L. & Nebert, D.

W. Comparison of oxidative stress response parameters in newborn mouse liver versus simian virus 40 (SV40)-transformed hepatocyte cell lines. *Biochem Pharmacol* **59**:703-712 (2000).
21. Larson, A. M. *et al.* Acetaminophen-induced acute liver failure: results of a United States multicenter, prospective study. *Hepatology* **42**:1364-1372 (2005).
22. Cohen, S. D. *et al.* Selective protein covalent binding and target organ toxicity. *Toxicol Appl Pharmacol* **143**:1-12 (1997).
23. Mirochnitchenko, O. *et al.* Acetaminophen Toxicity. Opposite effects of two forms of glutathione peroxidase. *J Biol Chem* **274**:10349-10355 (1999).
24. Canales, R. D. *et al.* Evaluation of DNA microarray results with quantitative gene expression platforms. *Nat Biotechnol* **24**:1115-1122 (2006).
25. Rico-Bautista, E., lores-Morales, A. & Fernandez-Perez, L. Suppressor of cytokine signaling (SOCS) 2, a protein with multiple functions. *Cytokine Growth Factor Rev* **17**:431-439 (2006).
26. Tanaka, S. *et al.* Grb7 signal transduction protein mediates metastatic progression of esophageal carcinoma. *J Cell Physiol* **183**:411-415 (2000).
27. Crabbe, J. C. *et al.* Elevated alcohol consumption in null mutant mice lacking 5-HT1B serotonin receptors. *Nat Genet* **14**:98-101 (1996).
28. Baurain, D., Dinant, M., Coosemans, N. & Matagne, R. F. Regulation of the alternative oxidase Aox1 gene in *Chlamydomonas reinhardtii*. Role of the nitrogen source on the expression of a reporter gene under the control of the Aox1 promoter. *Plant Physiol* **131**:1418-1430 (2003).
29. Villeneuve, D. J. *et al.* cDNA microarray analysis of isogenic paclitaxel- and doxorubicin-resistant breast tumor cell lines reveals distinct drug-specific genetic signatures of resistance. *Breast Cancer Res Treat* **96**: 17-39 (2006).
30. Liu, S. H. *et al.* Down-regulation of annexin A10 in hepatocellular carcinoma is associated with vascular invasion, early recurrence, and poor prognosis in synergy with p53 mutation. *Am J Pathol* **160**:1831-1837 (2002).
31. Keyse, S. M. & Emslie, E. A. Oxidative stress and heat shock induce a human gene encoding a protein-tyrosine phosphatase. *Nature* **359**:644-647 (1992).
32. Zimmers, T. A. Growth differentiation factor-15: induction in liver injury through p53 and tumor necrosis factor-independent mechanisms. *J Surg Res* **130**: 45-51 (2006).
33. Koizumi, H., Kartasova, T., Tanaka, H., Ohkawara, A. & Kuroki, T. Differentiation-associated localization of small proline-rich protein in normal and diseased human skin. *Br J Dermatol* **134**:686-692 (1996).
34. Belperio, J. A. *et al.* The role of the Th2 CC chemokine ligand CCL17 in pulmonary fibrosis. *J Immunol* **173**:4692-4698 (2004).
35. Turnley, A. M. Role of SOCS2 in growth hormone actions. *Trends Endocrinol Metab* **16**:53-58 (2005).
36. Hirabayashi, S. *et al.* JAM4, a junctional cell adhesion molecule interacting with a tight junction protein, MAGI-1. *Mol Cell Biol* **23**:4267-4282 (2003).
37. Fielden, M. R. & Zacharewski, T. R. Challenges and limitations of gene expression profiling in mechanistic and predictive toxicology. *Toxicol Sci* **60**:6-10 (2001).
38. Cabibbo, A., Consalez, G. G., Sardella, M., Sitia, R. & Rubartelli, A. Changes in gene expression during growth arrest of hepG2 hepatoma cells induced by reducing agents or TGBb1. *Oncogene* **16**:2935-2943 (1998).
39. Kim, B. H. *et al.* Expression profiling of actaminophen liver toxicity in mice using microarray technology. International symposium of the Korean society of toxicogenomics and toxicoproteomics. P-008, 111 (2004).